Quantum Chemical Semiempirical Approach to the Structural and Thermodynamic Characteristics of Fluoroalkanols at the Air/Water Interface

Yu. B. Vysotsky,[†] V. S. Bryantsev,[‡] F. L. Boldyreva,[§] V. B. Fainerman,[||] and D. Vollhardt*,[⊥]

Donetsk State University of Economics and Trade, 31 Shchorsa Str., 83050 Donetsk, Ukraine, Pacific Nortwest National Laboratory, Math Building, 906 Battelle Blvd, Richland, 99352, United States, Donbas Academy of Civil Engineering and Architecture, 2 Derzavina Str., 86123 Makiyivka, Ukraine, Medical Physicochemical Centre, Donetsk Medical University, 16 Ilych Avenue, 83003 Donetsk, Ukraine, and Max Planck Institute of Colloids and Interfaces, D-14424 Potsdam/Golm, Germany

Received: April 22, 2004; In Final Form: August 17, 2004

In the framework of quantum chemical PM3 approximation, the geometrical structure and thermodynamic functions characteristics of the formation of monomers ($n = 1-14, 34$), dimers ($n = 1-14, 34$), and trimers and tetramers ($n = 1-8$) of fluoroalkanols with the composition $C_nF_{2n+1}CH_2CH_2OH$ are calculated. It is shown that, in contrast to the fatty alcohols, which have a flat zigzag structure, the fluoroalkanol monomers are helical with an average backbone torsion angle equal to 162°. For the minimum-energy structure of dimers, the self-organization of the molecules in a dimer was observed; that leads to an opposite alternation of the torsion angles corresponding to the matching atoms in the two molecules that form the dimer. This results in the fact that the most stable conformation of the dimer is the double helix. The lead (39.5 Å) and diameter (7.3 Å) of the double helix are determined from the calculations of $C_{34}F_{69}CH_2CH_2OH$ dimers. Enthalpy, entropy, and Gibbs energy of the clusterization are shown to be linearly dependent on the length of the fluorinated chain. From the analysis of these thermodynamic quantities, it is concluded that dimerization of fluoroalkanols at the air/water interface takes place if the hydrocarbon link number exceeds 6, whereas for ordinary alcohols this characteristic number is 11. These calculated values agree with experimental data. The additive scheme for the evaluation of the clusterization free energies for arbitrary clusters is developed and applied to obtain the estimate of the Gibbs clusterization energy for infinitely large clusters.

1. Introduction

Quantum chemical calculations offer a way to obtain detailed information on intermolecular aggregates. The theoretical description of dimers and van der Waals molecules requires the correct account for the electrostatic, induction, and dispersion constituents of the interaction energy.[1,2] Ab initio molecular orbital calculations are becoming a powerful tool to study intermolecular interactions, provided that sufficiently extended basis sets and high level electron correlation corrections are incorporated.[3−8] However, at present these methods are capable of calculating only the lower homologues of various classes of compounds (e.g., alkanes,[3] fluoroalkanes,[4,5] and alcohols[6−8]). The adequate description of intermolecular interactions on the semiempirical level of the theory has been possible after the addition of different functions of the Gauss type to the basic core−core repulsion that may be considered as a van der Waals' attraction term (AM1 and PM3 methods).[9,10]

Earlier in the frame of the PM3 method, we calculated the structural and thermodynamic characteristics of the oligomerization and clusterization for the normal fatty alcohol series at the gas/liquid interface.[11−13] It has been shown that, for decanol and higher homologues, stable trimers are formed, whereas dodecanol and higher homologues are capable of forming not only trimers, but also infinite clusters. These results are in good agreement with the experimental data both in dependence of the thermodynamic characteristics of the clusterization on the number of methylene groups in the alcohol molecule and with regards to the morphologic structure of the clusters.

The experimental data for the compression of Langmuir monolayers of polyfluorinated alcohols also indicate the existence of a first-order phase transition.[14] It should be noted that quantum chemical calculations of the intermolecular interactions were made only for perfluoromethane,[4,5] perfluoroethane,[5] and hexafluoro-2-propanol[15] molecules, whereas the modeling of longer poly- and perfluoroalkanes were performed mainly using the force field method.[16−18] In the present study, a quantum chemical analysis of the structural and thermodynamic parameters of the dimerization (and the characteristics of trimers and tetramers) of the polyfluorinated alcohols $C_nF_{2n+1}CH_2CH_2OH$ with $n = 1-14, 34$ is performed, and these characteristics are compared with the corresponding values for ordinary alcohols and with the experimental results obtained for $C_8F_{17}CH_2CH_2$-OH.

2. Methods

Similarly to our previous publications,[11−13] the semiempirical calculations of monomers and dimers reported here were performed using the PM3 method implemented in the Mopac2000 software package.[19] Global geometry optimizations were performed with the Broyden−Fletcher−Goldfarb−Shanno optimization algorithm[19] because the default geometry optimizer,

[†] Donetsk State University of Economics and Trade.
[‡] Pacific Nortwest National Laboratory.
[§] Donbas Academy of Civil Engineering and Architecture.
[||] Donetsk Medical University.
[⊥] Max Planck Institute of Colloids and Interfaces.

10.1021/jp048240e CCC: $30.25
Published on Web 12/14/2004

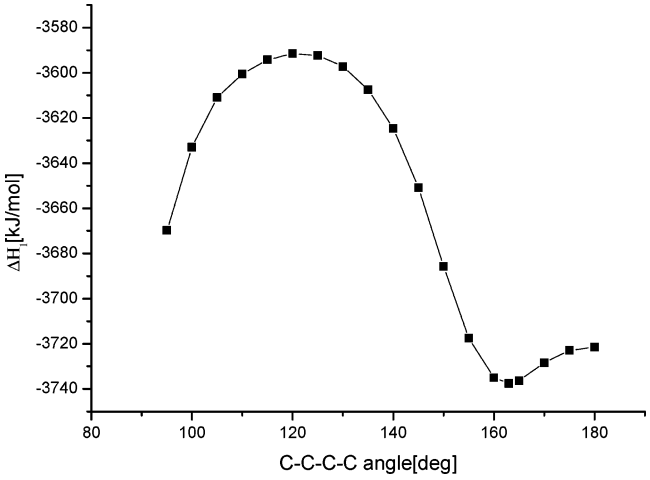

Figure 1. Conformational energy dependence for $C_8F_{17}CH_2CH_2OH$ on the backbone torsion angles.

Eigenvector Following, is unsuitable for large systems. Cartesian coordinates were used instead of the molecular coordinate system. This results in lower values of the optimized structures gradient norm, which is important for the calculations of the vibration frequencies and entropies. Standard entropy and Gibbs energy were estimated using the usual statistical thermodynamic equations with translation, rotational, and vibration terms.[19]

3. Experimental Section

The surface pressure−area (Π−A) isotherms were measured at different temperatures using a computer-interfaced film balance. The surface pressures measured with the Wilhelmy method using a roughened glass plate were reproducible to ±0.1 $mN \cdot m^{-1}$ and the areas per molecule to ±0.005 nm^2. The film balance was sheltered in a cabinet to avoid excessive disturbances by convection and contamination by impurities. After evaporating the spreading solvent, the molecules remaining at the air−water interface were continuously compressed and expanded at rates of 0.05 nm^2 $molecule^{-1}$ min^{-1}.

4. Results and Discussion

Monomers. The results of the calculations show that the geometric structure of fluoroalkanol monomers is essentially different from that of ordinary alkanols. Figure 1 illustrates the dependence of the conformational energy for $C_8F_{17}CH_2CH_2$-OH on the torsion angles between the carbon atoms. These angles were changed in steps of 5°, whereas all other geometric parameters were optimized. It is seen that, in contrast to the unbranched alkanols, which possess a zigzag structure, the plane geometric shape of the carbon framework for the $C_8F_{17}CH_2$-CH_2OH and its homologues corresponds to the maximum, not the minimum at the conformational curve (torsion angle 180°), whereas the helical conformation (torsion angle 162°) is energetically most preferable. The $C_{10}H_4F_{17}OH$ molecule is taken as an example for the geometrical structure of fluoroalkanols, presented in Figure 2a.

Note that the helical conformation exists also for perfluoroalkanes. This fact is evidenced both by experimental data[20] and quantum chemical calculations.[21,22] The helical distortion of the carbon framework is a common feature for these molecules and is probably caused by the mutual repulsion between the fluorine atoms. This conclusion is supported by the fact that subtracting the value of the F−F interaction between the nearest CF_2 groups calculated by the molecular mechanics approach from the total energy obtained in ab initio calculations leads to the value that is close to the energy of the corresponding hydrocarbon molecule (cf., e.g.,Volhardt and Fainerman[23]).

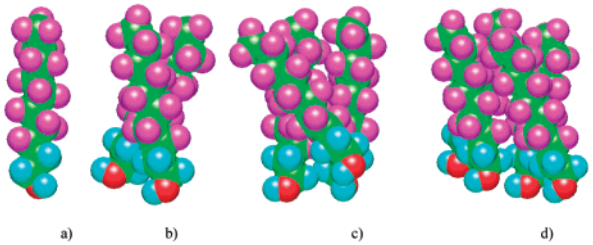

Figure 2. Molecular geometries of the most stable monomer (a), dimer (b), trimer (c), and tetramer (d) for the $C_8F_{17}CH_2CH_2OH$ molecule taken as an example.

TABLE 1: Geometrical Parameters of the $C_8F_{17}CH_2CH_2OH$ Monomer

geometrical parameters	MNDO	AM1	PM3	
bonding lengths, Å	$O-C_1$	1.39	1.41	1.40
	O−H	0.95	0.97	0.95
	C_1-C_2	1.56	1.52	1.53
	C_2-C_3	1.59	1.54	1.54
	C_3-C_4	1.68	1.62	1.61
	C_4-C_5	1.68	1.61	1.61
	C_9-C_{10}	1.68	1.62	1.61
	C_4-F	1.35	1.37	1.35
	C_3-F	1.35	1.37	1.36
	$C_{10}-F$	1.35	1.36	1.34
plane angles, degrees	HOC	112.2	107.5	107.7
	$C_1C_2C_3$	115.2	111.4	111.5
	$C_3C_4C_5$	114.4	110.6	110.6
	$C_7C_8C_9$	113.7	109.7	110.0
	$C_8C_9C_{10}$	113.8	109.8	109.5
	FC_3C_2	112.0	113.3	112.7
	FC_8C_7	109.4	110.4	110.3
	FC_9C_8	109.9	111.4	110.7
	$FC_{10}C_9$	111.4	112.3	111.9
torsion angles, degrees	$C_1C_2C_3C_4$	178.2	179.5	176.5
	$C_2C_3C_4C_5$	172.7	165.2	175.0
	$C_3C_4C_5C_6$	168.3	170.0	161.7
	$C_4C_5C_6C_7$	167.1	166.9	162.3
	$C_5C_6C_7C_8$	167.2	166.2	162.4
	$C_6C_7C_8C_9$	167.8	166.9	162.5
	$C_7C_8C_9C_{10}$	169.5	165.9	161.8

For the sake of comparison, we present in Table 1 the geometric parameters of the $C_8F_{17}CH_2CH_2OH$ monomer calculated using the MNDO, AM1, and PM3 methods. The results of the calculations show that the geometry of the fluoroalkanols is incorrect when it is calculated by MINDO/3. In some cases, instead of C−F bonds, unreal fragments with F−F−F bonds are obtained after the optimization of molecular structure. In MINDO/3 (contrary to MNDO, AM1, and PM3), the mutual repulsion of the fluorine atoms by the relevant atom−atom potentials is not taken into account. The carbon atoms in the chain are numbered according to the IUPAC rules. Comparing the results obtained in these calculations, one can see that all the methods above suggest the helical conformation as the most preferable one. The lowest deviation of the dihedral angle of the hydrocarbon chain from the value of 180° was obtained by the MNDO method, whereas the highest deviation was obtained in the PM3 calculations.

It should be stressed that the PM3 calculations for the fluorinated portion of the molecule lead to the best agreement with the ab initio results[23] for the perfluorinated butane, pentane, and hexane molecules (C−C bonding length 1.55 Å, CCC bonding angle 114−115°, CCCC torsion angle 162°, mean length of the CH_2 fragment 1.288 Å). Also, these data agree with the experimental results obtained by X-ray scattering of solid polyfluoroethylene.[20]

TABLE 2: Thermodynamic Characteristics for the $C_nF_{2n+1}CH_2CH_2OH$ ($n = 1-14, 34$) Series of Fluoroalcohol for $T = 298$ K

n	ΔH_1, kJ/mol	ΔS_1, J/mol·K	ΔG_1, kJ/mol
1	−905.28	356.31	−1011.46
2	−1310.75	416.36	−1434.82
3	−1712.19	469.89	−1852.22
4	−2117.86	520.15	−2272.87
5	−2523.08	572.20	−2693.62
6	−2927.67	623.54	−3113.48
7	−3333.77	675.05	−3534.94
8	−3738.07	726.55	−3954.59
9	−4144.34	778.68	−4376.38
10	−4548.47	829.56	−4795.66
11	−4954.94	881.44	−5217.62
12	−5360.25	932.28	−5638.11
13	−5765.59	983.45	−6058.64
14	−6170.86	1035.20	−6479.34
34	−14 272.80	2004.29	−14870.10

Comparing the geometric parameters of the $C_8F_{17}CH_2CH_2OH$ monomer calculated using the PM3 method with the corresponding parameters calculated for saturated *n*-alcohols, one can see that the fluorination of the hydrocarbon chain results in a slight decrease of the O−H and O−C bonding lengths, in an increase of the COH angle, and in some increase of the C−C bond nearest to the O−H bond (for fatty alcohols the O−H bonding length is 0.964 Å, the O−C bonding length is 1.415 Å, the C−C bonding length is 1.519 Å, and the COH angle is 107.3°). The distance between the fluorinated and unfluorinated carbon atoms (C_2-C_3) is somewhat larger than the C−C bonding length in fatty alcohols and alkanes. The bond between the carbon atoms of the fluorinated groups is essentially longer: the average length of the CF_2 fragment is 1.324 Å. This can be ascribed to the fact that the fluorine atoms are larger and repulsion exists between the fluorine atoms. Note that the helical structure of the monomer determines the values of dihedral angles of the hydrocarbon framework: in the fluorinated part of the molecule these angles are ca. 162°, in the protonated part this angle is 165°, and near the hydroxyl group the value is almost 180°, similarly to that in fatty alcohol molecules.

The calculated values of the thermodynamic parameters (enthalpy, ΔH, entropy, ΔS, and Gibbs energy, ΔG) for the $C_nF_{2n+1}CH_2CH_2OH$ ($n = 1-14, 34$) series for 298 K are listed in Table 2). Similarly to the unfluorinated alcohols,[12,13] the fluorinated alcohols also exhibit a dependence of the formation enthalpy and absolute entropy on the hydrocarbon chain length with large correlation coefficients:

$$\Delta H_1 = -(496.48 \pm 0.03) - (405.20 \pm 0.003)n, \quad (N = 11, R = 0.999, S = 0.030 \text{ kJ/mol}) \quad (1)$$

$$\Delta S_1 = (314.73 \pm 0.33) + (51.48 \pm 0.03)n, \quad (N = 11, R = 0.999, S = 0.3 \text{ J/mol·K}) \quad (2)$$

Here, N is the number of points, S is the standard deviation, and R is the correlation coefficient. Note that the two initial members of the homologous series are excluded from the correlation because their geometrical structures deviate essentially from that of the higher series members. Using eqs 1 and 2, one can predict the thermodynamic characteristics for the higher homologues of the series. For example, for the $C_{34}F_{69}CH_2CH_2OH$ molecule one obtains $\Delta H_1 = -14\,273.28$ (−14 272.82) kJ/mol and $\Delta S_1 = 2065.05$ (2004.29) J/(mol·K), where the values in parentheses are the results of the quantum chemical calculations. The fact is that the deviations between the values estimated from the correlation dependencies and those calculated explicitly is small and could possibly be ascribed to the deficiencies of the PM3 method if applied to the large spatial systems and caused by the presence of low-frequency vibrations in the vibrational spectra of such systems. Because the recent MOPAC versions disregard the frequencies below 100 cm^{-1}, which contribute most significantly to the vibrational entropy constituent, an additional procedure was developed to take these contributions into account.

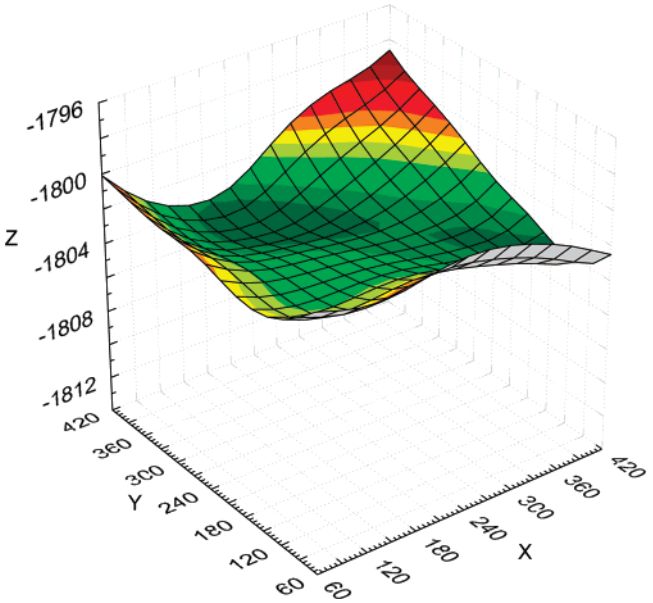

Figure 3. Potential energy surface for the $C_8F_{17}CH_2CH_2OH$ dimer. *Z* axis: standard formation enthalpy of the dimer [kJ/mol], *X* axis: φ [degree], *Y* axis: χ [degree].

Dimers. The existence of the helical structure in fluoroalkanols leads to their optical activity. Here, two types of dimers can be formed, with equal or opposite winding of the helixes. It should be also kept in mind that for each of these types of dimers several equilibrium configurations can exist. It was shown that, for a sufficiently high *n* value, n > 4, the interaction between the molecules with equal winding of the helixes is larger than for the molecules with opposite winding of the helixes. Therefore, in the present study only the results for the dimers formed by molecules with equal winding of helixes are presented.

With the $C_8F_{17}CH_2CH_2OH$ molecule taken as an example, possible equilibrium configurations (conformations) of dimers were considered, corresponding to various values of two rotation angles: the angle φ determining the rotation of the first monomer around its axis and the angle χ determining the rotation of the second monomer around the first one (around the same axis). Figure 3 shows the energy surface for the $C_8F_{17}CH_2CH_2OH$ dimer on φ and χ, which corresponds to minimum-energy points smoothed by the least-squares method. The angular dependence of energy a priori is the periodic function with the period equal to 2π; therefore, prior to the smoothing procedure this periodicity was imposed by the repeated surface profile in the range -3π to 5π along the angles (the unessential difference in the periodicity, apparent in Figure 3, is the result of smoothing). It is seen that two minima and maxima exist at the surface, which are separated by a saddle point. However, as for equally winded monomers, the rotation through an angle $\varphi = \varphi_1$ and $\chi = \chi_1$ is equivalent to the rotation through $\varphi = \chi_1$ and $\chi = \varphi_1$. These two minima correspond to the same structure of the dimer.

The molecular geometry of the most stable dimer is shown in Figure 2b. For this case, the distance l between the hydrogen and oxygen atoms in the OH groups is $l_{H-H'} = 6.28$ Å and $l_{O-O'} = 6.17$Å; the distance between the carbon atoms of two monomers is $l_{C1-C1'} = 5.63$ Å, $l_{C2-C2'} = 5.63$ Å, and $l_{C10-C10'} = 4.77$ Å; and the dihedral angles between the two monomers are $\angle C_4C_{4'}C_5C_6 = -84.9°$ and $\angle C_4C_{4'}C_{5'}C_{6'} = 88.9°$. It should be noted that the structural parameters of the dimer listed above almost do not depend on the monomer chain length (as expected, the most significant changes of these parameters were observed for the shortest chains). Therefore, it can be concluded that to locate the points of minima at the conformation surface for other values of the chain length it is unnecessary to perform quite time-consuming calculations for the entire surface; these points could be found from separate calculations starting from the minima determined earlier for a single value of the chain length.

We proceed next with the characterization of the geometric parameters of the monomers in fluoroalkanol dimers that are unrelated to the relative position of the monomers. It follows from the calculations that bonding lengths and valence angles of the monomers joined into dimers are quite the same as those in isolated monomers, whereas the dihedral angles between the carbon atoms undergo certain changes. Table 3 summarizes the calculated values of the dihedral angles between the atoms of the fluorinated carbon framework for each monomer in the dimer (φ_1 is the angle in the first dimer and φ_2 is the angle in the second dimer) as compared with corresponding angles in a noninteracting molecule. It is seen that in the bonded monomers the dihedral angles counted from atoms with even numbers are quite different from those counted from the atoms with odd numbers. To characterize these differences, the average values of dihedral angles ($\bar{\varphi}$) and their average quadratic deviations (S_0) are listed in the last row of Table 4. Whereas for the monomer $S_0 = 0.33°$, for the dimers S_0 increases from 4.54° for $C_7F_{15}CH_2CH_2OH$ to 5.92° for $C_{14}F_{29}CH_2CH_2OH$. Another feature is the increase of the average value of the dihedral angle in the dimers as compared to the noninteracting monomer. In other words, in our case the interaction between the molecules leads mainly to some unwinding of the helix. The $\bar{\varphi}$ and S_0 dependencies on the length of the fluorinated part of the molecular chain could be expressed, with a quite significant correlation coefficient ($R > 0.99$) by exponential expressions:

$$\bar{\varphi} = 166.27°/(1 + 0.0953 \exp(-0.316 \cdot n)) \quad (3)$$

$$S_0 = 5.98°/(1 + 10.00 \exp(-0.491 \cdot n)) \quad (4)$$

The numerators in eqs 3−4 correspond to the limiting values at infinite chain length. It is seen from Table 3 that the values for $n = 14$ are almost equal to these limits. Table 3 shows that the neighboring dihedral angles in the middle of the perfluorinated chain approach the values of 160.2 and 173.6°. It was mentioned earlier that the values of valence angles and bonding lengths are almost independent of *n*. Therefore, one can predict the geometry of the fluoroalkanol dimers for larger *n* values. Note also that the middle parts of the fluoroalkanol molecules match each other in such a way that the alternation of the dihedral angles that correspond to the atoms with equal numbers is opposite: for example, for $C_{14}F_{29}CH_2CH_2OH$ $\varphi_1(8,9,10,11) = \varphi_2(9,10,11,12)$, and, vice versa, $\varphi_2(8,9,10,11) = \varphi_1(9,10,11,12)$. It is possible that, at least for large *n* values, this self-organization of the monomers in a dimer leads to the fact that the dimer with similar winding of the monomer helixes is energetically more preferable as compared with the structure formed by oppositely winding helixes.

TABLE 3: Backbone Torsion Angles for Each Monomer in the Dimer

	$n = 7$		$n = 8$		$n = 9$		$n = 10$		$n = 11$		$n = 12$		$n = 14$		$n = 34$		
torsion angle φ	$\varphi 1$	$\varphi 2$	$\varphi 1$	$\varphi 2$	$\varphi 1$	$\varphi 2$	$\varphi 1$	$\varphi 2$	$\varphi 1$	$\varphi 2$	$\varphi 1$	$\varphi 2$	$\varphi 1$	$\varphi 2$	$\varphi 1$	$\varphi 2$	monomer
3, 4, 5, 6	167.4	159.9	167.6	160.1	167.5	160.3	167.5	160.4	167.4	160.5	167.4	160.5	167.3	160.5	167.3	160.6	161.5
4, 5, 6, 7	160.7	169.4	161.3	170.4	161.6	170.6	161.8	170.6	162.0	170.4	161.9	170.4	162.0	170.3	162.1	170.3	162.5
5, 6, 7, 8	169.8	160.0	171.7	159.3	172.8	159.7	173.1	159.9	173.0	160.2	172.9	160.3	172.7	160.3	172.7	160.4	162.2
6, 7, 8, 9	159.6	169.5	160.2	170.4	159.3	172.4	159.7	173.5	159.9	173.8	160.1	173.7	160.2	173.6	160.3	173.6	162.6
7, 8, 9, 10			169.7	159.5	170.4	160.2	172.3	159.3	173.5	159.6	173.7	159.8	173.6	160.1	173.4	160.2	162.3
8, 9, 10, 11					159.7	169.7	160.4	170.4	159.5	172.3	159.8	173.4	160.3	173.6	160.5	173.5	162.5
9, 10, 11, 12							169.6	159.8	170.3	160.5	172.2	159.6	173.6	160.2	173.3	160.5	162.4
10, 11, 12, 13									159.9	169.6	160.5	170.3	160.0	173.3	160.7	173.4	162.4
11, 12, 13, 14											169.6	159.9	172.2	159.7	173.3	160.6	162.4
12, 13, 14, 15													160.5	170.3	160.7	173.3	162.5
13, 14, 15, 16													169.6	159.9	173.3	160.6	161.7
average values of dihedral angles	164.54		165.02		165.35		165.59		165.77		165.90		166.9		166.70		162.27
average quadratic deviations	4.54		4.95		5.39		5.56		5.73		5.80		5.92		6.24		0.33

TABLE 4: Standard Thermodynamic Characteristics of Formation of $C_nF_{2n+1}CH_2CH_2OH$ Clusters Calculated with PM3 Approximation (ΔH_m and $T\,\Delta S_m^{cl}$ in kJ/mol, ΔS_m in J/mol·K)

n	ΔH_m	ΔH_m^{cl}	ΔS_m	ΔS_m^{cl}	$-T\,\Delta S_m^{cl}$	ΔG_m^{cl}
			dimer ($m = 2$)			
1	−1829.99	−19.43	555.48	−157.15	46.83	27.40
2	−2649.87	−28.38	655.68	−177.04	52.76	24.38
3	−3465.02	−40.64	759.53	−180.25	53.72	13.08
4	−4286.57	−52.00	847.16	−193.14	57.55	5.55
5	−5111.73	−66.95	932.01	−212.40	63.29	−3.65
6	−5934.95	−79.63	1021.74	−225.34	67.15	−12.48
7	−6756.80	−91.08	1112.25	−237.83	70.87	−20.21
8	−7577.94	−101.80	1203.43	−249.66	74.40	−27.40
9	−8398.93	−112.47	1293.57	−263.80	78.61	−33.86
10	−9220.00	−123.08	1383.74	−275.39	82.07	−41.01
11	−10 041.10	−133.92	1474.73	−288.15	85.87	−48.05
12	−10 862.30	−144.60	1564.74	−299.82	89.34	−55.25
13	−11 683.50	−155.43	1655.54	−311.36	92.78	−62.6
14	−12 504.60	−166.23	1745.29	−325.12	96.89	−69.34
34	−28 929.30	−383.65	3472.65	−535.93	159.71	−223.95
			trimer ($m = 3$)			
1	−2763.91	−48.07	759.02	−309.92	92.36	44.29
2	−4013.71	−81.47	880.98	−368.09	109.69	28.22
3	−5230.49	−93.93	1006.84	−402.84	120.05	26.12
4	−6468.37	−116.52	1149.89	−410.56	122.35	5.83
5	−7713.18	−146.01	1290.28	−426.33	127.05	−18.96
6	−8947.94	−164.95	1434.19	−436.43	130.06	−34.90
7	−10 195.20	−196.59	1540.83	−484.28	144.32	−52.27
8	−11 433.50	−219.24	1665.42	−514.21	153.23	−66.00
			tetramer ($m = 4$)			
1	−3690.48	−69.37	945.25	−480.01	143.04	73.68
2	−5334.51	−91.52	1161.43	−504.01	150.19	58.67
3	−6999.82	−151.06	1257.35	−622.21	185.42	34.36
4	−8644.44	−175.31	1443.74	−636.86	189.79	14.48
5	−10 317.20	−227.64	1611.33	−677.49	201.89	−25.74
6	−11 979.60	−268.96	1783.41	−710.75	211.80	−57.16
7	−13 659.50	−328.04	1935.21	−764.94	227.95	−100.09
8	−15 300.00	−347.67	2113.35	−792.81	236.26	−111.41

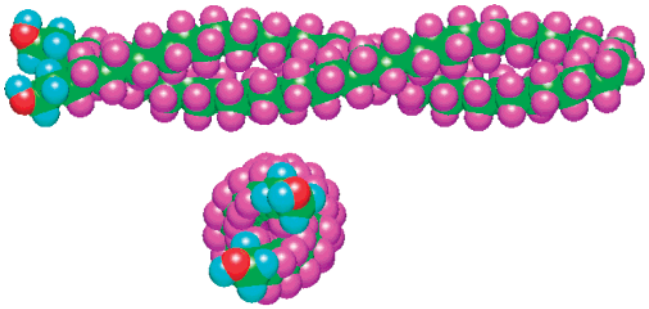

Figure 4. Double helix in the $C_{34}F_{69}CH_2CH_2OH$ dimer.

This self-organization results finally in the formation of a double helix; see Figure 4. To determine the dimensions of this helix more precisely, we performed calculations for the dimer with $n = 34$. It was found that the diameter of the double helix is 7.3 Å, whereas the monomer helix diameter is 3.34 Å; the lead of the double helix is 39.5 Å (33 fragments CF_2), whereas the monomer helix lead is 34.0 Å (28 fragments CF_2). The increase of the monomer helix lead in the dimer to a value of 39.5 Å should be ascribed to some unwinding of the helix during the supramolecular reorganization of the dimer, as explained above.

Table 4 summarizes the results of the calculation of standard formation enthalpy ΔH_2 and absolute entropy ΔS_2 of dimers for $C_nF_{2n+1}CH_2CH_2OH$ with $n = 1-14$, 34. In Table 4, enthalpy $\Delta H_2^{cl} = \Delta H_2 - 2\Delta H_1$, and entropy $\Delta S_2^{cl} = \Delta S_2 - 2\Delta S_1$ of the dimerization are also listed. It is seen that, similarly to the fatty alcohols, the values of enthalpy and entropy of dimers, and also the enthalpy and entropy of dimerization, become higher as n increases. As the values of ΔH_2^{cl} and ΔS_2^{cl} are negative, the corresponding contributions to the Gibbs energy are opposite by sign. Similarly to the fatty alcohol series, the following dependencies of these values on the chain length exist:

$$\Delta H_2^{cl} = -(11.18 \pm 1.51) - (11.16 \pm 0.16)\cdot n \text{ (N = 11, R = 0.999, S = 1.66 kJ/mol)} \quad (5)$$

$$\Delta S_2^{cl} = -(147.00 \pm 1.92) - (12.78 \pm 0.20)\cdot \text{n (N = 11, R = 0.999, S = 2.10 J/mol·K)} \quad (6)$$

Here, similarly to the expressions for the monomers, eqs 1 and 2 above, the first three members of the homologous series are omitted from the correlation. Using eqs 5 and 6, one can estimate the thermodynamic characteristics for higher members of the homologous series. For example, for the $C_{34}F_{69}CH_2CH_2$-OH dimer one obtains $\Delta H_2^{C1} = -390.62$ (−383.65) kJ/mol and $\Delta S_2^{C1} = 581.52$ (535.93) J/(mol·K), where the values in parentheses are the results of quantum chemical calculations.

Quite naturally, the slopes of eqs 5 and 6 describe the intermolecular interaction of the CF_2 groups, whereas the absolute terms correspond to the interaction of the OH and CH_2 groups. The additive scheme developed by Vysotsky et al.[13] for the description of the clusterization of normal fatty alcohols at the gas/liquid interface could be implemented for the description of the interaction between the unfluorinated parts of the fluoroalkanol molecules. The calculations performed according to this scheme yield the values of the absolute terms of eqs 5 and 6: for the dimerization enthalpy, −12.69 kJ/mol, and for the dimerization entropy, 146.6 J/(mol·K). These values

TABLE 5: Parameters of the Correlation Dependences for Enthalpy and Entropy of Oligomerization per Monomer

thermodynamic characteristics	correlation parameters	dimer	trimer	tetramer
ΔH_m^{cl}	a	-6.56 ± 0.46	-5.02 ± 2.02	-0.61 ± 5.25
	b	-5.46 ± 0.03	-8.53 ± 0.33	-11.13 ± 0.85
	S	0.89	1.04	2.70
	R	0.999	0.998	0.991
ΔS_m^{cl}	a	-80.07 ± 1.51	-98.41 ± 8.11	-119.24 ± 3.07
	b	-5.63 ± 0.11	-8.84 ± 1.32	-9.98 ± 0.50
	S	2.94	4.16	1.57
	R	0.998	0.968	0.996
ΔG_m^{cl}	a	17.30 ± 0.35	24.31 ± 2.27	34.92 ± 4.56
	b	-3.79 ± 0.03	-5.90 ± 0.37	-8.15 ± 0.74
	S	0.67	1.16	2.37
	R	0.999	0.994	0.989

are seen to be quite close to the values of the absolute terms of eqs 5 and 6, to within the standard errors of these coefficients. This enables one to describe fluoroalkanols possessing any number of CH_2 fragments. The fact that the standard errors for ΔH_2^{cl} and ΔS_2^{cl} are somewhat higher as compared with those obtained for unfluorinated compounds[13] could be possibly ascribed to the helical structure of the monomers. Note that, introducing the absolute terms of eqs 5 and 6 into the expression for the Gibbs energy, one can see that in the cases studied here the contributions from the unfluorinated parts of the molecules lead to a destabilization of the molecular cluster, $\Delta G > 0$. This fact corresponds well with the results reported by Cysotsky and co-workers,[11−13] where it was shown that, in agreement with the experimental data, stable clusters of fatty alcohols can be formed if the number of CH_2 groups exceeds 10.

Introducing eqs 5 and 6 into the expression for the free energy of dimerization:

$$\Delta G_2^{cl} = \Delta H_2^{cl} - T\Delta S_2^{cl} \quad (7)$$

and solving the inequality $\Delta G_2^{cl} > 0$ for standard conditions, one can see that for $n < 4.33$ dimers cannot be formed. It is seen from the comparison of the results presented here with those reported by Vysotsky et al.[13] that dimerization of fluoroalkanols can occur at a lower carbon framework length than dimerization of unfluorinated alcohols.

Trimers and Tetramers. In contrast to the situation with fatty alcohols for which the definition of initial unoptimized cluster structures for subsequent calculations using the PM3 method was quite straightforward, for fluoroalkanols that possess the helical structure the geometry of a cluster is far from obvious, thus making it necessary to consider all possible rotations of monomers. In this study, the most energetically advantageous monomers and dimers were taken as structural units. Similarly to the approach used for dimers, two rotation angles were also used in the calculations of the optimized geometry for larger structures: the angle of the dimer rotation around its axis and the angle of rotation of the remaining monomer (in the case of trimer) or dimer (in the case of tetramer) around its axis. Among 176 optimized structures of trimers and 230 optimized structures of tetramers, those most energetically advantageous were found; these are shown in Figures 2c and 2d for the $C_8F_{17}CH_2CH_2OH$ molecule taken as an example. The energy parameters of these clusters ($n = 1-8$) are listed in Table 4. It is necessary to note, that, using this method (two rotation angles), triple helices were not obtained.

It follows from the calculations of the geometric parameters of the studied clusters that, similarly to the case of dimers, bonding lengths and valence angles of monomers that constitute trimers and tetramers are almost the same as in isolated monomers, whereas the dihedral angles between the carbon atoms undergo more significant variations. The alternation of these angles is observed, which enables one to indicate structural units corresponding to dimers in the structure of trimers and tetramers. For example, in a trimer one of the monomers is almost unalternated (mean quadratic deviation is $S_0 = 1.03°$), whereas for the two other monomers in this trimer this parameter is close to that for an isolated dimer. Note that the formation of a trimer leads to the variation in the geometric parameters of both the monomer and the dimer. For example, the monomer helix becomes slightly unwounded (average value of the dihedral angle $\bar{\varphi} = 166.9°$, which is larger than in the isolated monomer), and the dimer double helix becomes slightly wounded ($\bar{\varphi} = 164.7°$) to match the monomer structure. The tetramer consists of two interacting dimers, each slightly unwounded ($\bar{\varphi} = 166.6°$) in comparison to the isolated dimers. This is illustrated in Figure 5, where matching of two dimers in the tetramer is clearly seen.

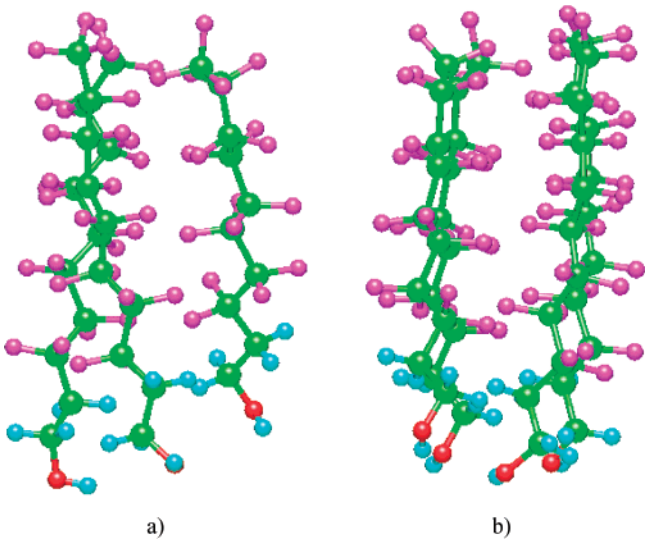

Figure 5. Structural units corresponding to dimers in the structure of trimers (a) and tetramers (b) for the $C_8F_{17}CH_2CH_2OH$ molecule taken as an example.

Similarly to the case of dimers, the correlations of enthalpy and entropy of clusterization ($\Delta H_m^{cl} = \Delta H_m - m\Delta H_1$ and $\Delta S_m^{cl} = \Delta S_m - m\Delta S_1$) with the CF_2 groups number in the monomer is observed; see Table 4. The parameters of these correlations ($x = a + bn$, $n = 4-8$) recalculated per one monomer are listed in Table 5. The dependencies of the thermodynamic characteristics of the cluster formation (dimer, trimer, and tetramer) per monomer on the number of CF_2 groups in the monomer are illustrated in Figure 6. Similarly to the case of fatty alcohols, the increase in the number of molecules in the cluster leads to the increase in the interaction energy per one monomer, which

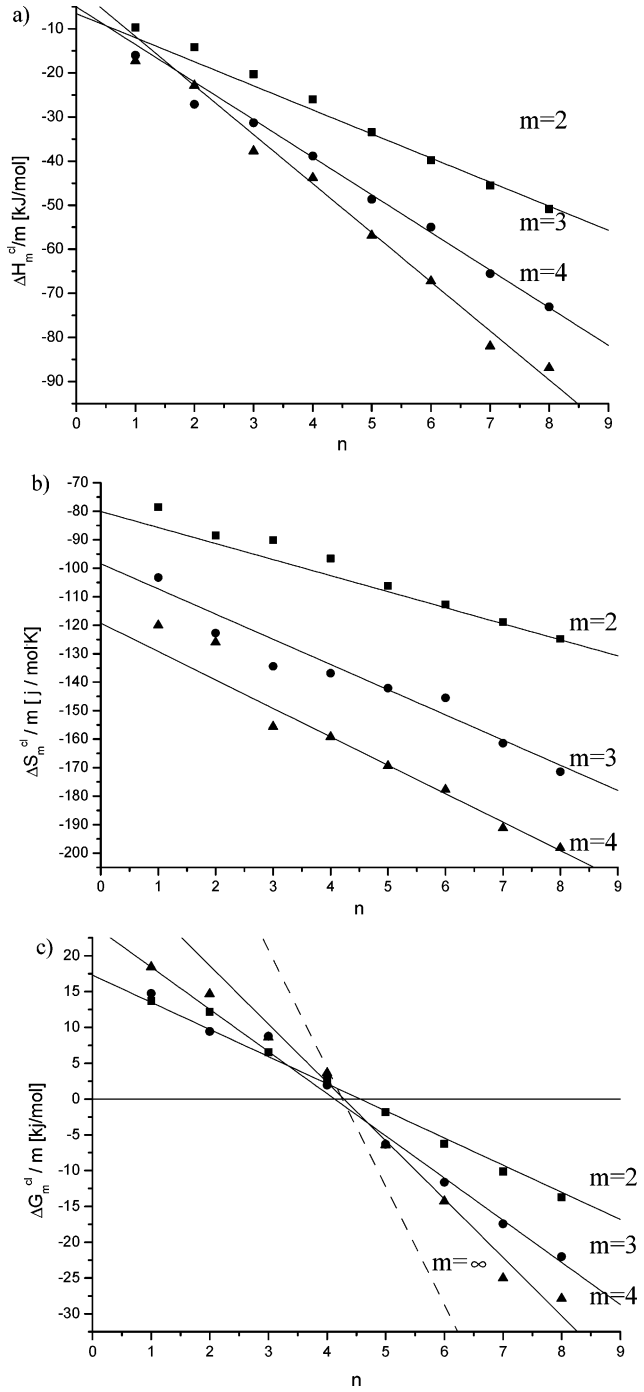

Figure 6. Dependence of the thermodynamic characteristics of cluster formation ((■) dimer, (●) trimer, (▲) tetramer) per monomer on the number of CF_2 groups in the monomer: (a) $\Delta H_m^{cl}/m$; (b) $\Delta S_m^{cl}/m$; (c) $\Delta G_m^{cl}/m$. The calculated dependence of $\Delta G_m^{cl}/m$ on n for an infinite square cluster is shown by dotted line.

results in the decrease in the cluster formation enthalpy $\Delta H_m^{cl}/m$. A similar dependence for the $\Delta S_m^{cl}/m$ is also observed. The dependence of the Gibbs clusterization energy value per one monomer on n is of particular interest; see Figure 6c. The horizontal straight line in this figure corresponds to the monomer. The fact that all straight lines intersect with each other in the $n = 3-5$ range shows that for $n > 5$ the increase of the cluster dimensions is thermodynamically favorable, whereas for $n < 3$ the clusters, if occasionally formed, should disintegrate into monomers. Similar behavior was also observed for fatty alcohols for $n > 9$.[13]

The energies of pair interactions between the monomers in the clusters were analyzed by removing one of each monomer

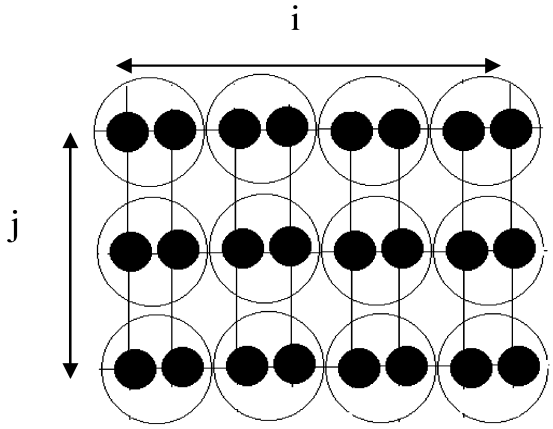

Figure 7. Schematic drawing of the rectangular cluster with dimensions $m = i \times j$. In this scheme the black circle is a monomer, the circle with two black circles inside is a dimer, i is the number of monomers along a horizontal line, and j is the number of monomers along a vertical line.

from the optimized trimer and subsequent single-point calculation of the energy of the remaining structure (geometry optimization was not performed). These calculations have shown that each trimer involves only two (not three) significant pair interactions, with the energy of each of these interactions being close to the dimerization energy. The energy of the third interaction (−9.6 kJ/mol) is lower than any of the energies of the first two interactions (−94.5 and −86.8 kJ/mol) by one order of magnitude. A similar analysis performed for the tetramer has shown the existence of four interactions approximately equal to each other, whereas diagonal pair interactions could be neglected. This fact, considered in conjunction with the geometric parameters of the clusters (see above) suggests that the dimers, which form ordered structures in tetramers and larger systems, should be regarded as structural units of which larger clusters are made. This enables one to predict the thermodynamic characteristics of plane clusters of any size.

Thus, Gibbs energy of the formation of an arbitrary m-cluster can be estimated. As the number of pair interactions, k, in the monomer, dimer, trimer, and tetramer is 0, 1, 2, and 4, respectively, then it could be expected that the absolute terms and slopes of the correlations ΔG_m^{cl} versus n for clusters with different m values (see Table 5) should linearly depend on k. In fact, such dependencies do take place: for the slope, the values are $R = 0.998$ and $S = 0.826$ kJ/mol, and for the absolute term $R = 0.9996$ and $S = 1.635$ kJ/mol. Therefore, for any arbitrary cluster the dependencies of ΔG_m^{cl} on the number n of CF_2 groups in the monomer and on the number of pair interactions between monomers, k, in the cluster are

$$\Delta G_m^{cl} = [(35.20 \pm 0.36) - (8.26 \pm 0.18)n]k \qquad (8)$$

Therefore, to determine the clusterization energy for an arbitrary cluster, one should particularize the specific cluster structure and calculate the number of pair interactions between the monomers in the cluster. This procedure is illustrated in Figure 7, where the rectangular cluster with dimensions $m = i \times j$ is considered as an example. In this scheme, the lines between the monomers correspond to the pair contacts. It is easily seen that the number of contacts for this cluster is

$$k = (i-1)j + (j-1)i = 2ij - (i+j) \qquad (9)$$

The expression for the Gibbs' clusterization energy per one

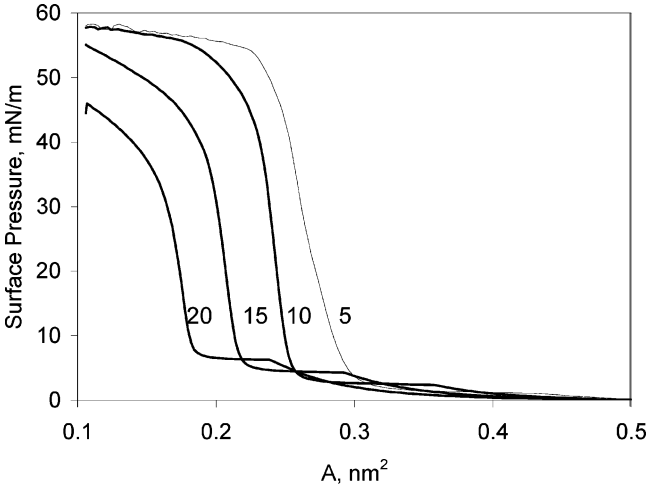

Figure 8. Surface pressure−area (Π−A) isotherms for $C_8F_{17}CH_2CH_2OH$ monolayers at different temperatures.

monomer is then

$$\Delta G_m^{cl}/m = [(35.20 \pm 0.36) - (8.26 \pm 0.18) \cdot n] \cdot [2 - i^{-1} - j^{-1}] \quad (10)$$

It is seen from this relation that for clusters with different geometries the limiting expressions corresponding to the infinite increase of the dimensions of a cluster are different. In particular, for the linear cluster ($j = 1$; $i \rightarrow \infty$), $\Delta G_m^{cl}/m = 35.20 - 8.26 \cdot n$; for linear chains ($j = 2$; $i \rightarrow \infty$), $\Delta G_m^{cl}/m = 52.80 - 12.39 \cdot n$ etc. To determine the structure of the most stable cluster consisting of a certain number of monomers, one should differentiate eq 10 at $i \times j = m$ with respect to i and set the resulting expression to zero; this yields the optimal lattice parameters of the two-dimensional cluster $i = j = \sqrt{m}$. Then, for the infinite square cluster ($j \rightarrow \infty$; $i \rightarrow \infty$), $\Delta G_m^{cl}/m = 70.4 - 16.52 \cdot n$. This dependence is shown by the dotted line in Figure 6c.

Comparison with experiment. The surface pressure−area (Π−A) isotherms for the $C_8F_{17}CH_2CH_2OH$ monolayers at various temperatures are shown in Figure 8. The experimental isotherms indicate that these systems undergo a first-order phase transition (from the fluid (gaseous, liquid expanded) to condensed monolayer state). Note that the monolayers of unfluorinated decanol do not exhibit any first-order phase transition. This transition was observed experimentally only for the dodecanol.[12,13] This result agrees with the calculations presented above. The displacement of the isotherms with the increase of the temperature shown on the left in Figure 8 is caused by the solubility of the $C_8F_{17}CH_2CH_2OH$. For insoluble monolayers in the fluid region, the dependence of the surface pressure on temperature is usually weak. This enables one to introduce approximate corrections for the solubility effect. The Π−A isotherms corrected by parallel shift are shown in Figure 9, together with the theoretical curves calculated from the thermodynamic model described earlier.[12,13,24] The model parameters are listed in Table 6, where ω_1 is the area per one monomer, A_c is the area corresponding to the onset of the phase transition, ϵ is the factor that accounts for the decrease of the area per one monomer in a cluster as compared to that in the unaggregated monomer, and m is the average clusterization degree in the fluid state. From the temperature dependence of these parameters, one can calculate the thermodynamic characteristics of clusterization.[12,13] For the formation of clusters from monomers, the values of thermodynamic parameters per one monomer calculated in this way are: $\Delta H_m^{cl}/m = -75.2$ (±12) kJ/mol, $\Delta S_m^{cl}/m = -242$ (±40) J/mol·K, and $\Delta G_m^{cl}/m = -(8 \pm 1)$ kJ/mol, which are quite close to those shown in Figure 6. The fact that the absolute experimental values of $\Delta G_m^{cl}/m$ and $\Delta H_m^{cl}/m$ are somewhat lower can be ascribed to experimental errors caused by the solubility of $C_8F_{17}CH_2CH_2OH$ in water (because the solubility leads to the decrease of the A_c/ω_1 ratio and, thus, to a decrease of the absolute value of $\Delta G_m^{cl}/m$).[12] Another factor that can lead to this inconsistency is the deficient account for the solvent influence in the procedure used to calculate $\Delta G_m^{cl}/m$ and $\Delta H_m^{cl}/m$.[12,13] It should be noted that by comparing the interaction energies of the CF_4 dimers calculated using the ab initio method (aug(df,pd)-6-311G** basis set)[5] with our PM3 results, one can see that a correlation between the corresponding interaction energy exists ($R = 0.99$, $S = 0.65$ kJ/mol). Whereas regarding geometrical and energetic characteristics, the results of the PM3 and ab initio calculations agree qualitatively and the PM3 method yields larger energy values. This can also lead to some differences between the experimental and theoretical values of Gibbs energy for the clusterization of fluoroalkanols.

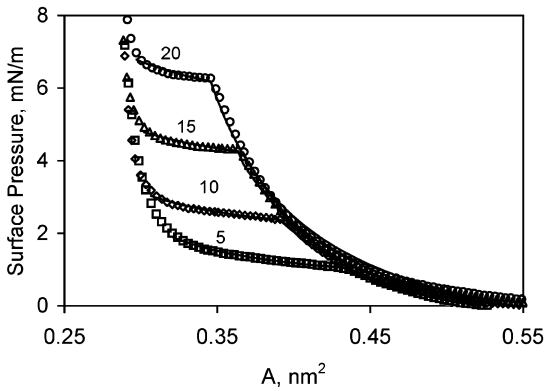

Figure 9. Corrected Π−A isotherms for $C_8F_{17}CH_2CH_2OH$ monolayers at different temperatures. The curves were calculated using the theoretical models in Vysotsky and co-workers.[12,13]

TABLE 6: Parameters of the Equation of State[12,13] for the Monolayers of $C_8F_{17}CH_2CH_2OH$

temperature, °C	5	10	15	20
ω_1, nm²	0.28	0.28	0.28	0.28
A_c, nm²	0.434	0.391	0.362	0.346
e	0.17	0.24	0.28	0.29
m	8.58	8.25	7.72	7.48

5. Conclusions

In the framework of PM3 molecular orbital approximation the thermodynamic function characteristics of the formation and geometrical structure of monomers, dimers, trimers, and tetramers of fluoroalkanols are calculated. It is shown that fluoroalkanol monomers possess a helical structure with an average backbone torsion angle equal to 162°, which implies optical activity of these molecules and the existence of two types of dimers, dimers with equal and opposite directions of helixes winding. For the minimum-energy structure of a dimer, corresponding to the equal winding direction of the monomer chains, self-organization of the monomers in the dimer is shown to take place with opposite alteration of the dihedral angles corresponding to the atoms with the same numbers in different dimer molecules. The double helical structure is the most preferable dimer structure. The lead (39.5 Å) and diameter (7.3 Å) of the double helix was determined from the calculation of $C_{34}F_{69}CH_2CH_2OH$ dimers. Enthalpy, entropy, and Gibbs energy of

the clusterization are linearly dependent on the fluorinated chain length. From the calculations, it follows that dimerization of fluoroalkanols at the air/water interface takes place for carbon chain lengths exceeding 6, whereas for ordinary alcohols the value corresponding to the dimerization onset is 11. These facts agree with the experimental data. An additive scheme for the evaluation of the free energy of clusterization for clusters with arbitrary length is developed. This scheme is used to estimate the Gibbs energy of the clusterization for some infinite rectangular clusters.

References and Notes

(1) Hobza, P.; Zahradnic, R. *Intermolecular Complexes. The Role of van der Waals Systems in Physical Chemistry and in Biodisciplines*; Academia Praga: Prague, 1988.

(2) Stone, A. J. *The Theory of Intermolecular Forces*, International Series of Monographs on Chemistry 32; Clarendon Press: Oxford, 1996.

(3) Metzger, T. G.; Ferguson, D. M.; Glauser, W. A. *J. Comput. Chem.* **1997,** *18*, 70.

(4) Para, R. D.; Zeng, X. C. *J. Mol. Struct. (THEOCHEM)* **2000**, *503*, 213.

(5) Tsuzuki, S.; Uchimaru, T.; Mikami, M.; Urata, S. *J. Chem. Phys.* **2002**, *116*, 3309.

(6) Hagemeister, F. C.; Gruenloh, C. J.; Zwier, T. C. *J. Phys. Chem. A* **1998**, *102*, 82.

(7) Zimmermann, D.; Haber, T.; Schaal, H.; Suhm, M. A. *Mol. Phys*. **2001**, *99*, 413.

(8) Huelsekopf, M.; Ludwig, R. *J. Mol. Liq*. **2000**, *85*, 105.

(9) Dewar, M. J. S.; Zoebish, E. G.; Heally, E. F.; Stewart, J. J. P. *J. Am. Chem. Soc*. **1985**, *107*, 3902.

(10) Stewart, J. J. P. *J. Comput. Chem*. **1989**, *2*, 209.

(11) Vysotsky, Yu. B.; Bryantsev, V. S.; Fainerman, V. B.; Vollhardt, D.; Miller, R. *Colloids Surf., A* **2002**, *209* 1.

(12) Vysotsky, Yu. B.; Bryantsev, V. S.; Fainerman, V. B.; Vollhardt, D.; Miller, R. *J. Phys. Chem. B* **2002**, *106*, 121.

(13) Vysotsky, Yu. B.; Bryantsev, V. S.; Fainerman, V. B.; Vollhardt, D. *J. Phys. Chem. B* **2002**, *106*, 11285.

(14) Takiue, T.; Vollhardt, D. *Colloids Surf., A* **2002**, *198*−*200* 797.

(15) Schaal, H.; Haber, T.; Suhm, M. A. *J Phys. Chem. A* **2000**, *104*, 265.

(16) Byutner, O. G.; Smith, G. D. *Macromolecules* **2000**, *33*, 4264.

(17) Sprik, M.; Rothlisberger, U.; Klein, M. L. *J Phys. Chem. B* **1997**, *101*, 2745.

(18) Cui, S. T.; Siepmann, J. I.; Cochran, H. D.; Cumminds, P. T. *Fluid Phase Equilib.* **1998**, *146* 56.

(19) Stewart, J. J. P. *MOPAC 2000.00 Manual*; Fujitsu Limited: Tokyo, Japan, 1999.

(20) *Polymer Handbook*; Brandrup, J., Immergut, E. H., Eds.; Wiley-Interscience: New York, 1989.

(21) Smith, G. D.; Jaffe, R. L.; Yoon, D. Y. *Macromolecules* **1994**, *27*, 3166.

(22) Watkins, E. K.; Jorgensen, W. L. *J. Phys. Chem. A* **2001**, *105*, 4118.

(23) Holt, D. B.; Farmer, B. L.; Macturk, K. S.; Eby, R. K. *Polymer* **1996**, *37*, 1847.

(24) Vollhardt, D.; Fainerman, V. B. *J. Phys. Chem. B* **2004**, *108*, 297.